

Polymer Chain Shape of Poly(3-alkylthiophenes) in Solution Using Small-Angle Neutron Scattering

Bryan McCulloch,^{†,§} Victor Ho,[†] Megan Hoarfrost,[†] Chris Stanley,[‡] Changwoo Do,[‡] William T. Heller,[‡] and Rachel A. Segalman^{*,†,§}

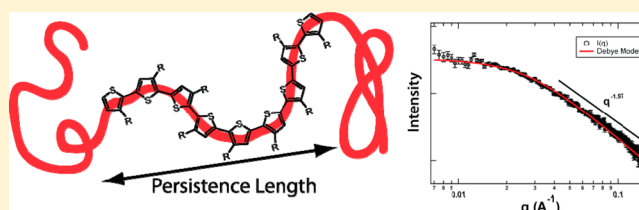
[†]Department of Chemical and Biomolecular Engineering, University of California, Berkeley, Berkeley, California 94720-1462, United States

[‡]Biology and Soft Matter Division, Oak Ridge National Laboratory, Oak Ridge, Tennessee 37831, United States

[§]Materials Science Division, Lawrence Berkeley National Laboratory, Berkeley, California 94720, United States

Supporting Information

ABSTRACT: The chain shape of polymers affects many aspects of their behavior and is governed by their intramolecular interactions. Delocalization of electrons along the backbone of conjugated polymers has been shown to lead to increased chain rigidity by encouraging a planar conformation. Poly(3-hexylthiophene) and other poly(3-alkylthiophenes) (P3ATs) are interesting for organic electronics applications, and it is clear that a hierarchy of structural features in these polymers controls charge transport. While other conjugated polymers are very rigid, the molecular structure of P3AT allows for two different planar conformations and a significant degree of torsion at room temperature. It is unclear, however, how their chain shape depends on variables such as side chain chemistry or regioregularity, both of which are key aspects in the molecular design of organic electronics. Small-angle neutron scattering from dilute polymer solutions indicates that the chains adopt a random coil geometry with a semiflexible backbone. The measured persistence length is shorter than the estimated conjugation length due to the two planar conformations that preserve conjugation but not backbone correlations. The persistence length of regioregular P3HT has been measured to be 3 nm at room temperature and decreases at higher temperatures. Changes in the regioregularity, side chain chemistry, or synthetic defects decrease the persistence length by 60–70%.



INTRODUCTION

Delocalization of electrons along the backbone of conjugated polymers leads to their interesting electronic properties as well as the potential for substantially increased backbone stiffness. Electron delocalization favors a planar conformation between neighboring monomers and has been shown to lead to rodlike behavior and liquid crystallinity in many of these materials.^{1,2} The flexibility of conjugated polymers controls many of their fundamental properties such as their mechanical and optoelectronic properties and also impacts phenomena such as crystallization and self-assembly behavior (micelles, block copolymers, etc.).³ Classical polymers have very flexible backbones because many possible configurations are populated; however, intermolecular interactions such as sterics, hydrogen bonding, and Coulombic interactions can also affect chain stiffness. The chain shape of conjugated polymers has important ramifications on charge transport along the chain axis, and structural defects such as hairpin turns have been shown to represent breaks in conjugation.⁴ In bulk materials, intermolecular packing can further impact intermolecular charge transport, excited state energetics, and crystallization.^{5,6} Delocalization of electrons along the backbone, in combination with steric interactions, leads to a unique mechanism affecting the chain shape in conjugated polymers and these interactions

are relevant in understanding the complex morphological behavior (phase separation, crystallization, and molecular orientation) observed in optoelectronic devices such as organic photovoltaics, light-emitting diodes, and transistors.

Even though conjugated polymers tend to be relatively rigid, there exists a wide range of observed persistence lengths for conjugated polymers due primarily to differences in sterics caused primarily by side chain interactions, conjugation lengths due to different degrees of electronic delocalization, and geometric factors such as the bond angles between monomers. The chain shape of conjugated polymers has primarily been studied using dilute solution light scattering. For example, poly(2-methoxy-5-(2'-ethylhexyloxy)-*p*-phenylenevinylene) (MEH-PPV) has a conjugated backbone and exhibits a relatively high degree of stiffness with a measured persistence length around 6 nm.^{7,8} After the addition of large bulky side groups, the persistence length of PPV derivatives can be increased to over 40 nm by sterically favoring the planar trans conformation.^{7,8} Optical single molecule spectroscopy of conjugated polymers, pioneered by Barbara and co-workers,

Received: November 29, 2012

Revised: January 23, 2013

Published: February 19, 2013

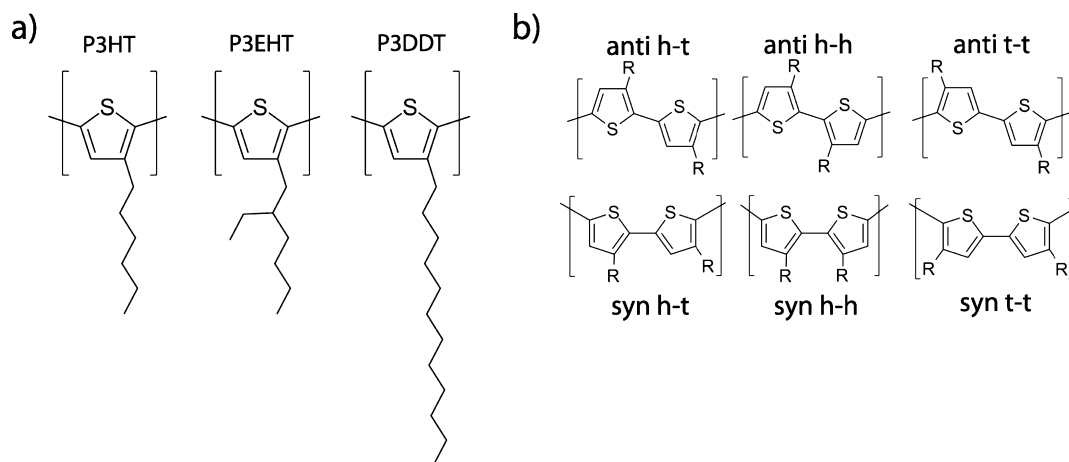


Figure 1. (a) Polythiophenes of different alkyl side chains (P3HT, P3EHT, and P3DDT) have been examined in this study. (b) Polythiophene monomers can adopt two primary conformations. The anti conformation is energetically preferred to the syn conformation. Regioregularity, which is controlled synthetically, is associated with the position of the side chain on thiophene rings of adjacent monomers and influences the possible backbone conformations. The head-to-tail coupling (h-t) produces less steric hindrance than the head-to-head (h-h) and tail-to-tail (t-t) couplings.

has also been used extensively to understand the conjugation length and arrangement of chromophores in conjugated polymers by dispersing a dilute concentration of conjugated polymers in an inert polymer matrix such as PMMA.⁴ While this technique does not directly measure the chain shape of a polymer, it gives information about the orientation of chromophores within a molecule and can be used to model the polymer chain shape. Work done on MEH-PPV has shown that these chains are semiflexible and do not follow a random walk statistics. Instead, chains aggregate or fold upon themselves due to their strong intramolecular π -stacking interactions.⁹ In the case of MEH-PPV, it has been suggested that the flexibility of these materials has been shown to be related to structural defects such as hairpin turns and chemical defects which cause a break in conjugation.¹⁰ Similar to MEH-PPV, polyfluorene (PF) has a long persistence length of around 7 nm measured in dilute solution by light scattering.¹¹ The persistence length of PF is also limited by a combination of finite backbone torsion and nonzero bond angles between monomers leading to a polymer which is relatively stiff but would still undergoes a random walk at high molecular weights. Poly(*p*-phenylene) (PPP) is unique because this conjugated polymer has a single bond angle of 0° between monomers which leads to a long persistence length of around 28 nm even though there is significant backbone torsion between monomers and thus a shorter conjugation length.^{12–14} Conjugated polymers typically do not achieve comparable persistence lengths to extremely stiff polymers such as DNA (50–70 nm)¹⁵ because there are typically two possible conformations (e.g., *cis/trans*) that preserve planarity, and a significant amount of backbone torsion often exists since electron delocalization can actually tolerate some torsion along the backbone without being significantly affected.

Poly(3-alkylthiophenes) (P3ATs) represent one of the most studied classes of conjugated polymers due to their high hole mobility and a relatively low bandgap; however, it is still unclear how rigid these polymers are and how the persistence length of these polymers is affected by factors such as side chain chemistry or regioregularity. P3ATs have two possible monomer conformations shown in Figure 1. Both the anti and syn conformations preserve conjugation along the backbone by retaining the planar geometry; however, the anti

confirmation is the lower energy state and is the only confirmation that would produce a rigid polymer backbone.¹⁶ Without any torsion between monomers, the backbone geometry would resemble a two-dimensional random walk from a distribution of anti and syn planar conformations. Flexibility of the P3AT backbone, which leads to a three-dimensional polymer structure, comes from a distribution of syn and anti conformations as well as a finite amount of torsion between monomers.

The degree of flexibility in P3ATs has been discussed in many studies; however, there exist a wide range of estimates for the persistence length, and it is unclear what influences the chain shape of these materials. Furthermore, this wide range of persistence lengths makes it unclear whether P3ATs should be thought of as being a rodlike polymer. The first studies into the chain shape of P3ATs were carried out by Aime et al. on poly(3-butylthiophene) (P3BT) in nitrobenzene using small-angle neutron scattering.^{17,18} They found that the persistence length of P3BT was around 5.5 nm; however, there was scattering at low angles due to chain aggregation which may have obscured the single polymer chain form factor. They also measured an increase in the persistence length to over 85 nm when doping with NOSbF_6 attributed to increased electron delocalization. Heffner et al. used static light scattering and dilute solution viscometry to look at poly(3-hexylthiophene) (P3HT) and poly(3-octylthiophene) (P3OT) in THF and found that the persistence length of these materials was around 2.1–2.4 nm. These initial studies used FeCl_3 -catalyzed polymerizations which results in polymers with high polydispersity and relatively low regioregularity and may contain coupling defects along the backbone and catalytic impurities which may dope the polymer chain.^{19,20} After the development of new synthetic techniques, the chain shape of regioregular P3HT was first studied by Yamamoto et al. using static light scattering where it was suggested that the persistence length may be as high as 30 nm.²¹ Single chain spectroscopy of dilute P3HT mixtures in a PMMA film showed that the chromophores in regiorandom P3HT are more disordered than regioregular P3HT, suggesting that the chain shape may be more flexible for regiorandom P3HT.²² There have also been theoretical predictions of the persistence length of P3ATs using molecular dynamics simulations which predicted

persistence lengths as high as 86 nm but showed a large decrease of around 25% for regiorandom polymers.²³ Conversely, recent work on regioregular poly(3-(2'-ethyl)hexylthiophene) (P3EHT) block copolymers in the disordered melt using small-angle X-ray scattering combined with mean-field random phase approximation theory estimated the persistence length to be around 6 nm.²⁴ There are several explanations for such a wide range of observed values including differing synthesis techniques, solvents, side chain chemistry, regioregularity, and measuring techniques. For example, strong light absorption over a wide range of wavelengths can make static light scattering difficult in polythiophenes. It is also important to note that P3ATs have strong intermolecular interactions which can cause polymer chain aggregation, even at low concentrations, which can make it difficult to extract single chain statistics. Studying the chain shape using small-angle neutron scattering for polythiophenes in the melt, as well as other rodlike or conjugated polymer systems, has been difficult because these polymers suffer from a large amount of low- q scattering caused by long-range correlations which overwhelms single chain scattering.²⁵

Previous studies have shown that there is a wide range of measured and predicted persistence lengths for P3ATs. This may be caused by effects from regioregularity, synthetic defects, side chains, and experimental difficulties measuring the persistence length. Polymer synthesized through FeCl_3 catalyzed routes or polymer with low regioregularity may have drastically different persistence lengths because of backbone defects or increased backbone torsion compared to the high regioregularity polymers synthesized today using the GRIM and Rieke methods. The side chain may also affect the polymer chain shape of P3ATs. For PPV derivatives a bulky side chain leads to a stiffer polymer because it favors the trans conformation; however, in P3ATs as the side chain increases in volume, the backbone torsion may also increase, leading to a less rigid backbone. In this work, we set out to systematically investigate the effect of regioregularity, side chain chemistry, synthetic route, solvent choice, and temperature on the chain shape of P3ATs. Neutron scattering experiments show P3ATs follow random coil statistics, and while the backbone conjugation does impart some degree of stiffness, the measured persistence lengths are in the range where these materials should be thought of as semiflexible and not rodlike.

EXPERIMENTAL SECTION

Materials. Chemicals were purchased from Sigma-Aldrich and used without further purification unless otherwise noted. Poly(3-hexylthiophene) (P3HT), poly(3-(2'-ethyl)hexylthiophene) (P3EHT), and poly(3-dodecylthiophene) (P3DDT) were synthesized by standard procedures from the literature via Grignard metathesis polymerization (GRIM).^{26,27} P3HT and P3EHT were also synthesized by standard procedures from literature via a FeCl_3 -catalyzed polymerization.²⁸ While the ethylhexyl side chain of P3EHT contains a chiral center, a racemic mixture of monomers was used. All monomers were prepared according to standard procedures.²⁶ Polymers were precipitated in methanol, purified by Soxhlet extraction, dried, and stored under vacuum away from light. Regiorandom P3HT and Rieke P3DDT were purchased from Sigma-Aldrich.

Polymer Characterization. A Malvern triple detector gel permeation chromatography system was used to measure the absolute molecular weight and absolute molecular weight distribution of these polymers. A representative absolute molecular weight distribution is shown in Figure 2. This technique utilizes an inline refractive index detector, viscometer, and low angle light scattering detector (Malvern TDA 302 detector array) to access the absolute molecular weight

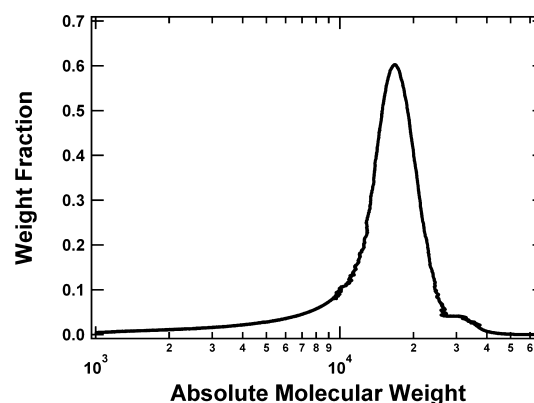


Figure 2. Absolute molecular weight distribution of P3HT-1 obtained by triple detector GPC.

distribution of a polymer. A single monodisperse polystyrene standard (Polymer Source) of known concentration was used to measure the refractive index, viscometer, and light scattering detector responses of the system.²⁹ THF was used as the mobile phase at a flow rate of 1 mL min^{-1} , and Waters Styragel HR2, HR4, and two HR3 columns were used.

^1H NMR spectra were measured on a Bruker AVQ-400 spectrometer using deuterated chloroform solutions. Molecular weights were confirmed by end-group analysis from the ^1H NMR spectra. NMR was also used to confirm the chemical composition of the final product and to calculate the polymer regioregularity. Because of signal-to-noise limitations and peak broadness, it was difficult to ascertain differences between samples with very high degree of regioregularity. The density of these polymers was measured using a density gradient column (glycerin/isopropanol) to estimate the monomer volume. The monomer volume of P3HT was estimated to be 0.300 nm^3 , P3EHT was estimated to be 0.388 nm^3 , and P3DDT was estimated to be 0.466 nm^3 . A reference volume of 0.1 nm^3 was assumed for statistical segment length calculations common with convention. UV-vis absorbance measurements between 350 and 900 nm using dilute polymer solutions in dichlorobenzene were made with a Varian Cary 50 instrument.

Small-Angle Neutron Scattering. Small-angle neutron scattering (SANS) studies were conducted at the extended Q-range small-angle neutron scattering diffractometer (EQ-SANS BL-6) line at the Spallation Neutron Source (SNS) located at Oak Ridge National Laboratory (ORNL). A sample-to-detector distance of 4 m was used,

Table 1. Characteristics of Polymer Samples

polymer	synthetic route	M_n^a (kg/mol)	PDI ^a	regioregularity (%)
P3HT-1	GRIM	15.1	1.17	>97
P3HT-2	GRIM	7.4	1.08	>97
P3HT-3	regiorandom	40.7	1.92	58
P3HT-4	FeCl_3 oxidation	63.9	2.42	79
P3EHT-1	GRIM	10.0	1.13	>97
P3EHT-2	GRIM	10.2	1.24	>97
P3EHT-3	GRIM	18.4	1.44	>97
P3EHT-4	GRIM	4.8	1.07	>97
P3EHT-5	GRIM	20.1	1.33	>97
P3EHT-6	GRIM	12.1	1.35	>96
P3EHT-7	FeCl_3 oxidation	38.0	1.90	80
P3DDT-1	GRIM	22.9	1.32	>96
P3DDT-2	GRIM	32.0	1.34	>96
P3DDT-3	Rieke	33.4	1.57	>96

^aBased on the absolute molecular weight distribution measured by triple detector GPC.

and the instrument was operating in 60 Hz frame-skipping mode with a minimum wavelength, λ , setting of 2.5 Å, providing two wavelength bands (2.5–6.1 and 9.4–13.4 Å).³⁰ Data reduction followed standard procedures implemented in MantidPlot. The measured intensity was corrected for detector sensitivity and the scattering contribution from the solvent and empty cells, azimuthally averaged into $I(q)$ vs q ($q = 4\pi \sin(\theta)/\lambda$, where 2θ is the scattering angle) and placed on an absolute scale using a calibrated standard.³¹ Samples were dissolved at a concentration of 2–5 mg mL⁻¹ in deuterated solvent and stirred overnight. A range of concentrations were measured to confirm the absence of significant interchain interactions which would cause low q scattering. Titanium sample cells with quartz windows and a 1 mm path length were used.

SANS Intensity Modeling. The scattering contrast in SANS originates from different scattering cross sections of the deuterated solvent and the nondeuterated polymer chains. By operating in the dilute polymer limit where polymer chains are not interacting, SANS can be used to extract information related to correlations along a single polymer chain. Most polymer chains can be estimated to undergo a random walk and follow Gaussian chain statistics. For a random coil, the Debye function can be used to model the scattering of a single chain:

$$g(u) = \frac{2}{u^2}(u - 1 + e^{-u}) \quad (1)$$

where u is given by

$$u = q^2 R_g^2 = q^2 \left(\frac{b^2 N}{6} \right) \quad (2)$$

and R_g is the radius of gyration of the polymer chain.³² For a polymer undergoing a random walk, R_g can be replaced with an expression including b , the statistical segment length, and N , which is the number of monomers in the chain. Both the statistical segment length (b) and the degree of polymerization (N) are calculated using the reference volume of 0.1 nm³. This equation is derived to correspond to monodisperse polymer chains and for the remainder of this paper will be referred to as the standard Debye model.

The scattering intensity of a polymer can be fit using the following equation:

$$I(q) = Kg(q) + I_{\text{inc}} \quad (3)$$

where K is a scaling factor, $g(q)$ is the form factor of a single chain, and I_{inc} is the incoherent scattering intensity which is assumed independent of q . In theory, the scaling factor can be predicted from the scattering intensity, concentration, and polymer molecular weight. However, in this analysis K has been treated as a fitting parameter to account for any errors in the absolute intensity calibration and because the amorphous density of P3ATs is not well-known. There are only three fitting parameters in the resulting model: the incoherent background scattering intensity (I_{inc}), the scaling factor (K), and the statistical segment length of the polymer (b) if the polymer molecule weight is known.

The standard Debye model has been used successfully despite the finite polydispersity of most polymers. If the molecular weight distribution follows an ideal distribution, the standard Debye model can be analytically corrected,³³ but molecular weight distributions are often nonideal and cannot be represented by a simple function. To correct the standard Debye model for the effects of polydispersity, it is possible to numerically integrate the single chain scattering over the entire molecular weight distribution (using triple detector GPC as shown in Figure 2) using the following function:

$$I(q) = K \int_{N=0}^{N=\infty} w_i g(u_{N_i}) N_i dN_i + I_{\text{inc}} \quad (4)$$

where w_i is the weight fraction at a particular molecular weight, N_i is the degree of polymerization, and $g(u_{N_i})$ is the standard Debye model evaluated at N_i .³⁴ Similar to the standard Debye model, K and I_{inc} have

been treated as fitting parameters. The model in eq 4 will be referred to as the polydispersity-corrected Debye model.

While the Debye model for Gaussian coils should fit well for high molecular weight polymers, deviations occur when the polymer contour length is less than or roughly equal to the persistence length. This occurs for low molecular weight polymers or relatively rigid polymers. The Debye model is also unable to fit data at high q values when the length scale probed begins to behave rodlike. The wormlike chain model is able to account for these effects and for this work the approximate form for single chain scattering formulated by Sharp and Bloomfield is used:

$$g(u) = \frac{2}{u^2}(u - 1 + e^{-u}) + \frac{2}{5q^2 L^2} [4u - 11ue^{-u} + 7(1 - e^{-u})] \quad (5)$$

where L is the contour length of the chain ($L = nl_0$, where n is the number of thiophene monomers per chain and l_0 is the contour length of each thiophene monomer).³⁵ It is important to note that n is the actual number of thiophene rings per chain and is not normalized by a reference volume. For P3ATs, l_0 corresponds to the length of one monomer and is taken to be 0.39 nm, confirmed by theory and crystallography.^{18,36} For the wormlike chain model there is also a more complex form for R_g leading to the following expression:

$$u = q^2 R_g^2 = q^2 \left[\frac{Ll_p}{3} - l_p + \frac{2l_p^3}{L} \left(1 - \frac{l_p}{L} + \frac{l_p}{L} e^{-L/l_p} \right) \right] \quad (6)$$

where l_p is the persistence length.³⁷ This expression can be corrected for finite polydispersity similar to the polydispersity corrected Debye model shown above by integrating over the molecular weight distribution in a similar manner with the following equation:

$$I(q) = K \int_{n=0}^{n=\infty} w_i g(u_{n_i}) n_i dn_i + I_{\text{inc}} \quad (7)$$

While the form of this equation is more complicated, it still contains only three fitting parameters which is the same number as in the standard Debye model. Experimental uncertainty in the measured scattering intensity and molecular weight distribution has also been propagated through this analysis.

While both the statistical segment length and persistence length quantify the polymer chain shape, they give different values and fundamentally describe slightly different but related quantities. The statistical segment length is derived to describe the distance between uncorrelated random walks within a Gaussian coil. The persistence length describes the decay in directional correlations between monomers along the polymer backbone. The statistical segment length is normalized to the monomer volume of the polymer and a chosen reference volume (chosen to be 0.1 nm³).³⁸ This makes it useful when comparing between polymers of different chemistry; however, the absolute statistical segment length depends on the chosen reference volume. The monomer volume also depends on the density of the amorphous polymer which has been estimated and is a source of uncertainty. In comparison, the persistence length depends on the monomer length which is well-known and ties the value for the persistence length directly to the length over which the backbone is rigid, an unambiguous physical parameter. The rest of the discussion will therefore focus primarily on the use of the wormlike chain model and the derived persistence length from this model. It is important to note that it is possible to easily convert between the persistence length and statistical segment length when the polymer behaves as a random coil ($L \gg l_p$) because the expression for R_g of a wormlike chain collapses to

$$R_g^2 = \frac{1}{3} Ll_p = \frac{1}{3} l_0 l_p n \quad (8)$$

and through algebraic manipulation the following expression can be used to convert between l_p and b :

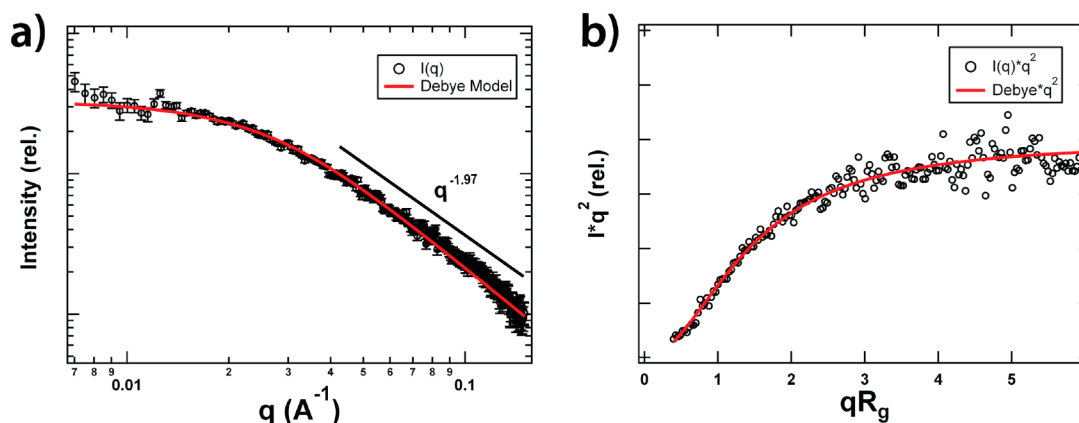


Figure 3. (a) Small-angle neutron scattering (SANS) of P3HT-1 (after incoherent scattering subtraction) in dichlorobenzene shows that P3ATs adopt a random coil chain shape with a scaling of $I \approx q^{-2}$ over a large region corresponding to a Gaussian coil. (b) A Kratky plot shows the typical plateau which also indicates a random coil which can be fit using the Debye model.

$$l_p = \frac{\nu_m b^2}{\nu_r 2l_0} \quad (9)$$

where ν_m is the monomer volume and ν_r is the reference volume (chosen to be 0.1 nm^3).³⁸ Therefore, throughout the text both the persistence length and statistical segment length are provided for each model; however, a Gaussian coil is assumed when converting between persistence length and statistical segment length. Since the contour length of the polymers studied is always much longer than the persistence length, this assumption should be valid.

The characteristic ratio is also a useful parameter in describing the chain shape of these materials and is defined as

$$C_\infty = \frac{\langle R^2 \rangle}{l_0^2 n} = \frac{\nu_m b^2}{\nu_r l_0^2} = \frac{2l_p}{l_0}$$

for a Gaussian coil. The characteristic ratio represents the size of a polymer chain, normalized by the size of the polymer chain if each monomer underwent a random walk and therefore can be thought of as the actual polymer chain size compared to the smallest possible size it could occupy if each monomer underwent a new step in a random walk.

DISCUSSION

Representative small-angle neutron scattering curves of P3HT in dichlorobenzene (d-DCB) are shown in Figure 3. All polymer samples show similar scattering patterns with slight variations due to changes in molecular weight and persistence length. The scattering intensity scales as $q^{-1.96 \pm 0.08}$ which indicates that the polymer chain adopts a random coil geometry and is consistent with the conformation of a polymer chain in a theta solvent or a polymer melt. If the Porod scaling deviated from q^{-2} , it would be an indication that the chain shape architecture may not be well described as a random coil. The intensity scaling remains near q^{-2} for all solvent and polymer combinations studied, and the Debye model, derived for a Gaussian coil, can be fit to a wide region of the scattering pattern. The Kratky plot in Figure 3b also shows a scattering pattern consistent with a Gaussian coil conformation. At high q values the intensity should scale like a rigid rod (as q^{-1}) because at high q , length scales less than the persistence length are being probed. Unfortunately, the scattering intensity at high q was insufficient to analyze due to the low polymer concentration, low scattering contrast, and relatively low molecular weight used in these studies.

Polythiophenes (and other conjugated polymers or rodlike polymers) have strong intramolecular interactions and poor solubility, often leading to an upturn in scattering at low q values.^{17,18} This can obscure the scattering from isolated chains and makes it difficult to extract useful chain shape statistics. By using reasonably low molecular weight polymers, low concentrations, and solvents with high P3AT solubility, the amount of low- q scattering has been decreased, and it is only apparent at the lowest q values ($<0.008 \text{ \AA}^{-1}$). For these systems it is much more reliable to fit a model to the entire data set than to try to use Guinier's law at low q to extract the polymer radius of gyration. Guinier analysis does give radius of gyration consistent with our findings; however, since it can be difficult to choose the relevant q range, these data has not been included.

The standard Debye model assumes monodisperse polymer chains which is a sufficient assumption for P3ATs polymerized using GRIM with polydispersities ranging from 1.05 to 1.3 for most polymers. As shown in Figure 4 and Table 2, all models used fit the data quite well; however, correcting for polydispersity causes subtle changes in the predicted intensity

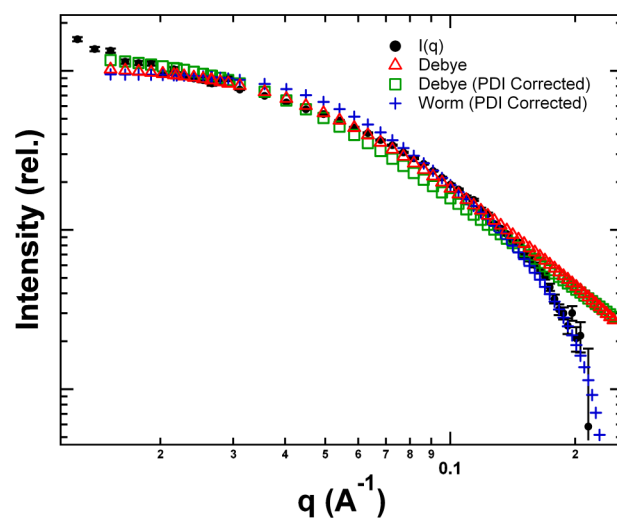


Figure 4. Scattering from P3EHT-4 can be described well using any of the above models; however, the wormlike chain model is more consistent at high q values where the length scale approaches the persistence length and the polymer no longer behaves like a random coil.

Table 2. Comparison of Chain Shape Parameters from the Debye, Wormlike Chain, and Polydispersity-Corrected Models for Regioregular Polymers Synthesized via GRIM

polymer	solvent	Debye	Debye PDI corrected		wormlike chain PDI corrected	
		b (nm)	b (nm)	l_p (nm)	b (nm)	l_p (nm)
P3HT	d-DCB	0.8 ± 0.1	0.9 ± 0.1	3.0 ± 0.3	0.9 ± 0.5	2.9 ± 0.1
P3EHT	d-DCB	0.8 ± 0.1	0.8 ± 0.1	2.9 ± 0.2	0.8 ± 0.6	3.0 ± 0.1
P3EHT	d-toluene	1.2 ± 0.1	0.8 ± 0.1	3.1 ± 0.2	0.9 ± 0.4	3.3 ± 0.2
P3DDT	d-DCB	0.7 ± 0.1	0.5 ± 0.1	1.1 ± 0.1	0.5 ± 0.4	1.6 ± 0.1
P3DDT	d-toluene	0.8 ± 0.1	0.6 ± 0.1	1.4 ± 0.1	0.5 ± 0.8	1.5 ± 0.1

because the range of molecular weights broadens the transition between the low q plateau ($\sim 0.01\text{--}0.04 \text{ \AA}^{-1}$) and the random coil Porod scattering regime at higher q ($\sim 0.1\text{--}0.2 \text{ \AA}^{-1}$). The wormlike chain model results in the highest quality fit because it is able to account for scattering at high q ($\sim 0.2 \text{ \AA}^{-1}$) by modeling the rodlike nature of the polymer backbone at short length scales. Even though the wormlike chain model fits slightly better than the Debye model, they both provide equally valid information about the polymer chain shape because the Debye model is not derived to fit at high q . Since the contour length of these polymers is much greater than the persistence length (or statistical segment length), these polymers behave as random coils leading to similar results between the PDI corrected Debye and wormlike chain models. Therefore, either model can be used to describe the chain shape of these polymers. For the remainder of the discussion, the PDI-corrected wormlike chain model will be used because the model offers more reliable fits since it operates over a larger range of length scales.

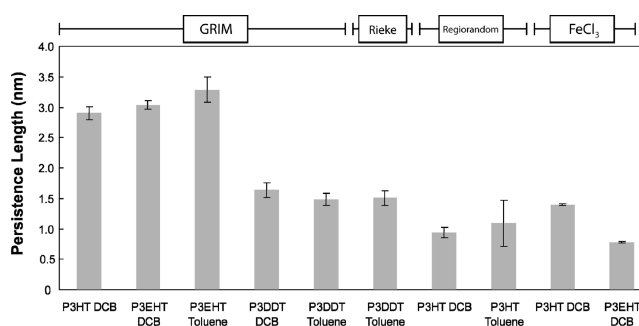
Table 2 shows that the solvent choice between d-DCB and d-toluene does not significantly affect the chain shape. While the solubility of P3EHT and P3DDT is higher in d-DCB than d-toluene, both solvents have high polymer solubility and the difference in solvent quality may not be enough to change the chain shape of these materials. The Porod intensity in d-DCB scales as $q^{-2.00 \pm 0.09}$ compared to P3ATs in d-toluene which scale as $q^{-1.95 \pm 0.07}$. It is interesting that these materials maintain the same q^{-2} scaling, which indicates that the polymer chains adopt a random coil and not swollen chain architecture. While dichlorobenzene is one of the best solvents that exist for these polymers, it may not have sufficiently favorable interactions to alter the chain conformation, which is consistent with what is known about P3AT's strong intermolecular interactions. This is in contrast to classical polymers in good solvents where solvent-polymer interactions are more favorable than polymer-polymer interactions such that the chain prefers to maximize solvent-polymer contact.

As seen in Table 3 and Figure 5, the persistence length of regioregular P3HT and P3EHT is 3.0 ± 0.1 nm. This is significantly longer than the persistence length of a flexible polymer such as polystyrene ($l_p = 0.92$ nm)³⁹ or polyisoprene ($l_p = 0.43$ nm).⁴⁰ The characteristic ratio of these materials is also relatively high ($\sim 12\text{--}14$), much greater than polyethylene (~ 6.8), but only slightly more than the characteristic ratio for polystyrene (~ 10.8).⁴¹ It does not appear to affect the chain shape whether P3ATs are synthesized by GRIM or Rieke synthetic routes since both of these methods result in high regioregularity polymers with little to no defects.

There are at least three major factors that affect the chain shape in these materials: side chain chemistry, regioregularity, and possibly synthetic defects along the backbone. There is a large decrease ($\sim 50\%$) in the persistence length between P3HT

Table 3. Comparison of Chain Shape Parameters from the Wormlike Chain Model for Different Polymers and Solvent Conditions

polymer	synthetic route	solvent	l_p (nm)	C_∞
P3HT	GRIM	d-DCB	2.9 ± 0.1	12.1 ± 1.0
P3EHT	GRIM	DCB	3.0 ± 0.1	13.3 ± 1.0
P3EHT	GRIM	d-toluene	3.3 ± 0.2	13.4 ± 1.3
P3DDT	GRIM	d-DCB	1.6 ± 0.1	8.0 ± 1.3
P3DDT	GRIM	d-toluene	1.5 ± 0.1	7.2 ± 1.2
P3DDT	Rieke	d-toluene	1.5 ± 0.1	7.3 ± 1.2
P3HT	regiorandom coupling	d-DCB	0.9 ± 0.1	4.7 ± 0.8
P3HT	regiorandom coupling	d-toluene	1.1 ± 0.4	5.4 ± 2.0
P3HT	FeCl ₃ oxidation	d-DCB	1.4 ± 0.1	7.0 ± 1.0
P3EHT	FeCl ₃ oxidation	d-DCB	0.8 ± 0.1	3.8 ± 0.6

**Figure 5.** Comparison of the persistence length from the wormlike chain model shows that P3AT chain shape appears to be a function of side chain chemistry and regioregularity for the polymers examined.

or P3EHT and P3DDT. This is likely due to steric interactions between side chains that causes either backbone torsion and/or a different population between the syn and anti conformations. From previous theoretical studies, short side chains should not dramatically affect the energetics associated with backbone conformations; however, long side chains may have an effect on the polymer chain shape.^{42,43} UV-vis absorbance spectra can be used to examine the conjugation length of these materials to try to elucidate which of these effects is more important in these materials. Backbone torsion results in an increase in the optical band gap (shorter conjugation length) and decreased persistence length. Both the syn and anti conformations are planar, and these conformations maintain conjugation along the backbone so a change in the distribution of syn and anti states alters the persistence length without affecting the conjugation length. The UV-vis spectrum, shown in Figure S1, indicates that P3DDT possesses a conjugation length nearly equal to P3HT. This indicates that the long side chain may not be causing increased backbone torsion in P3DDT. Instead, the fraction of monomers in the syn conformation increases which lowers the persistence length while maintaining a constant

conjugation length. The syn conformation may be lower in energy for P3DDT than in P3HT or P3EHT because the syn conformation plays the side chains apart, increasing the volume of which a side chain can occupy for very long side chains. For short side chains, the syn conformation has more steric hindrances than the anti conformation because the side chains are closer together, and it is the higher energy conformation. Conversely, the conjugation length of P3EHT is slightly shorter than that of P3HT despite the fact that persistence length is unchanged. This indicates that the branched side chain close to the backbone may lead to a slight increase in backbone torsion. The steric interactions in P3EHT occur close to the polymer backbone and may slightly favor the anti conformation because it is less sterically hindered than the syn conformation for a short bulky side chain. It is possible that P3EHT could have a slightly higher population of anti conformations, but this effect is offset by the slight increase in backbone torsion, resulting in a relatively unchanged persistence length compared to P3HT.

Regioregularity also was observed to dramatically decrease the persistence length of these materials. The persistence length of P3HT was decreased around 67% between highly regioregular P3HT and regiorandom P3HT. Regioregularity has been known to have strong effects on interchain interactions and chain packing affecting properties such as crystallinity.⁵ It also should affect the intrachain interactions by introducing large steric hindrances, possibly causing backbone torsion and a different distribution of syn and anti conformations.⁴² The conjugation length of regiorandom P3HT is the lowest of the polymers studied which may suggest that there exists a higher level of backbone torsion in these materials (Figure S1).

Finally, the persistence length of P3HT and P3EHT synthesized using the historically relevant FeCl_3 -catalyzed reaction is reduced by a similar amount as regiorandom P3HT. This is slightly surprising because these polymers are around 80% regioregular, and we may have expected their persistence lengths to be somewhere between that of regioregular and regiorandom P3AT. This synthesis is much less specific than the other synthetic routes studied and can result in polymers that have defects along the chain where the backbone is coupled through the 4-position rather than the 5-position on the thiophene ring.^{19,20} These defects could lead to increased steric hindrance or larger effective bond angles consistent with the lower observed conjugation length. It also appears that the branched side chain of P3EHT leads to a greater decrease in the persistence length than in P3HT when both are synthesized via the FeCl_3 synthetic route, but it is unclear if this is due to a difference in intramolecular interactions caused by the side chain or a change in defect concentration arising during the synthesis of these materials.

The chain shape of polymers can be thought of as depending on the bond angle and degree of backbone torsion between monomers. The chain shape of a polymer can be described using the freely rotating chain model assuming fixed bond angles and no restrictions on torsion angles. The persistence length for a freely rotating chain can be estimated using the following equation:

$$l_p^{\text{FRC}} = \frac{l_0}{2} C_\infty^{\text{FRC}} = \frac{l_0}{2} \left(\frac{1 - \cos \theta}{1 + \cos \theta} \right)$$

where l_0 is the monomer length (0.39 nm) and θ is the bond angle between monomers. For polythiophenes, the bond angle

between monomers has been estimated to be 121.1° ⁴⁴ and leads to a predicted persistence length of 0.61 nm. This estimate is very low, and the error in this estimate originates from the fact that polythiophenes have two conformational states that are energetically preferred, leading to a planar structure, and therefore do not occupy all torsion angles equally.

Instead, the chain shape can be better described using the hindered rotation chain model which can take into account conformations of differing energetics:

$$l_p^{\text{HRC}} = \frac{l_0}{2} C_\infty^{\text{HRC}} = \frac{l_0}{2} \left(\frac{1 - \langle \cos \phi \rangle}{1 + \langle \cos \phi \rangle} \right) \left(\frac{1 - \cos \theta}{1 + \cos \theta} \right)$$

where θ is the bond angle between monomers and ϕ is the torsion angle of rotation about the backbone of a monomer relative to its neighbor as shown in Figure 6.⁴⁵ For the syn

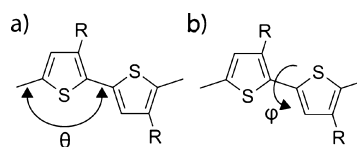


Figure 6. (a) Bond angle (θ) between monomers has been calculated to be around 121° and is assumed to be relatively fixed. The torsion angle (ϕ) varies between 0° for the syn conformation and 180° for the anti conformation shown above. The torsion angle between monomers can vary from these conformations; however, this will affect the delocalization of electrons and impact the conjugation length.

conformation $\phi = 0^\circ$ and for the anti conformation $\phi = 180^\circ$. The energy difference between these states has been calculated theoretically to be around 0.05 eV for a bithiophene molecule.^{42–44} To compute the average population as a function of angle, a Boltzmann distribution is assumed. If only the syn or anti conformations are allowed and no other backbone torsion angles are considered, 86% of the monomers are in the anti conformation at room temperature, and P3AT should have a persistence length of 3.8 nm. It is unlikely that backbone torsion is absent because polythiophenes have broad energy wells centered at 0° and 180° , and therefore the distribution of backbone torsion should be accounted for. The energy was assumed to scale as the degree of overlap between the p-orbitals of the thiophene monomers that should scale roughly as $\cos^2 \phi$. The barrier height for rotation of polythiophene has been experimentally and theoretically predicted to be around 0.18 eV.^{42,43,46} Using this simple model to include the effects of backbone torsion, we estimate the persistence length to be around 3.2 nm, which agrees fairly well with our experimental observations. Backbone torsion is important but a smaller effect than the distribution of syn/anti conformations on the persistence length of regioregular P3ATs. Regiorandom P3ATs will have a different energy landscape because of increased steric interactions leading to shorter persistence lengths.⁴² While this model can account for the effect of bond angles and backbone torsion between adjacent monomers, it is unable to account for long-range interactions such as excluded volume or sterics which may also be important in predicting the chain shape of P3ATs.

If the amount of backbone torsion is increased in P3ATs, the persistence length and conjugation length should decrease. Thermochromism exists in P3ATs, and it has been shown that the optical band gap increases as temperature increases.^{16,47} By

increasing temperature, the amount of backbone torsion should increase and the distribution of syn and anti conformations along the backbone should also change. Since the difference in energy of the syn and anti conformations is around $1.8k_B T$ at room temperature, the persistence length of these materials should be relatively strongly temperature-dependent. As shown in Figure 7, both the estimated conjugation length and the

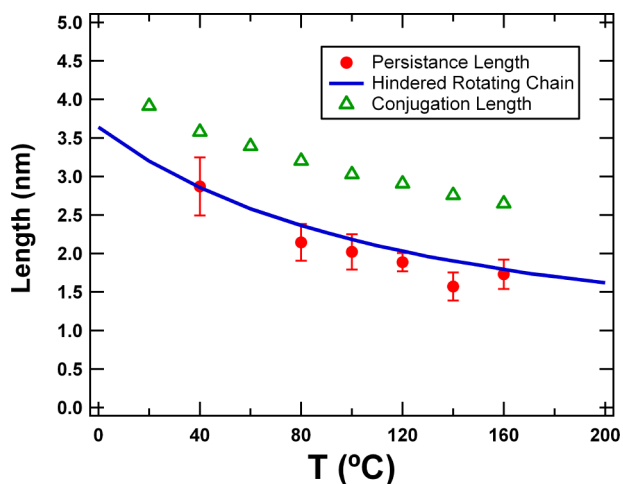


Figure 7. Persistence length of P3HT in d-DCB decreases as a function of temperature. This trend can be predicted using the hindered rotating chain model and energetic predictions from the literature. The conjugation length (calculated from the optical band gap)^{12,49,50} decreases as a function of temperature; however, it is always greater than the persistence length.

measured persistence length decrease as temperature is increased, with the measured persistence length decreasing by around 40% between 40 and 160 °C. Also presented in Figure 7, the decrease is remarkably well described by the hindered rotating chain using no fitting parameters. This suggests that the rotational energetics that describes a bithiophene molecule may translate to P3HT and that the sterics of the hexyl side chain may not dramatically affect the conformations of this polymer. Instead, the energetics related to the delocalization of electrons along the polymer backbone is responsible for its relatively stiff backbone. The temperature dependence of P3ATs with varying side chains or regioregularity may be different because of the increased steric interactions. This observed temperature-dependent behavior is in contrast with most polymer persistence lengths which typically are not strong functions of temperature. In traditional polymers, the difference in energy between the possible conformations is often much less than $k_B T$, and the energy wells associated with these conformations may be much steeper than P3ATs since the energetics for many polymers are dominated by steric interactions. Polystyrene, for example, shows no change in the chain shape over a similar temperature range because all possible conformations are accessible at room temperature.⁴⁸ Interactions between the solvent and polymer chain may also be temperature dependent, causing a change in chain shape; however, the Porod intensity scaling in this study does not change as a function of temperature.

The decrease in the conjugation length as a function of temperature demonstrates that the backbone torsion increases with temperature. It is not known how the conjugation length is exactly related to the average torsion angle; however, the

persistence length drops by 20% more than the conjugation length between 40 and 160 °C, which shows that the persistence length is more sensitive to temperature than the conjugation length in P3HT. While it is clear that the backbone conjugation accounts for strong intramolecular interactions in P3ATs, the measured conjugation length for conjugated polymers is not necessarily a good indicator of the chain stiffness in conjugated polymers. In poly(phenylenevinylene) and polyfluorene the conjugation length is usually less than the persistence length.^{8,11,12,51} In these cases the steric interactions make one of the two possible planar conformations very unfavorable, resulting in stiff polymers. The electronic structure of these polymers limits the conjugation length of these materials and is dramatically affected by chain stiffness. In P3HT, the opposite trend is observed where the average conjugation length is 3.8 nm, which is around 25% higher than the measured persistence length.^{12,49,50} This apparent disagreement can be reconciled by the fact that both the syn and anti conformations preserve the conjugation but do not maintain the spatial backbone correlations. Poly(phenylenevinylene) and polyfluorene only have one, highly populated planar conformation, making them very stiff; however, they possess a small degree of backbone torsion which limits the conjugation length. Polythiophenes also have backbone torsion which limits the conjugation length and have two populated planar states which preserve conjugation leading to a longer conjugation length than persistence length.

Interchain interactions in the melt may cause deviations from the values derived from dilute solution experiments; however, theoretically the persistence lengths of polymers in dilute solution should be similar to the persistence lengths calculated in the melt if the polymer solutions are near the theta solvent condition.⁴⁸ Efforts were made to study these materials in the melt; however, low- q scattering prevented analysis even for P3AT samples which were isotropic melts. It is unclear what the source of this large low- q scattering is; however, it must be caused by correlations over large length scales and probably has origins similar to the low- q scattering seen in rodlike or liquid crystalline polymers.²⁵

CONCLUSIONS

The chain shape of P3ATs in solution have been measured using small-angle neutron scattering and can be described using the Debye model and the wormlike chain model. These materials adopt a random coil geometry and have a semiflexible backbone with a persistence length around 3 nm for regioregular P3ATs. The side chain chemistry, regioregularity, and synthetic route can have an impact on the persistence length, decreasing it by as much as ~60–70%. Using the known molecular geometry and a simple model for the intramolecular interactions, the persistence length of P3ATs and their temperature dependence are consistent with experimentally measured values. The flexibility of the backbone arises from the distribution of syn and anti conformations as well as significant backbone torsion in polythiophenes. This results in a shorter persistence length than the estimated conjugation length, opposite of many other common conjugated polymers.

ASSOCIATED CONTENT

Supporting Information

Figures are included showing UV–vis absorbance maxima, concentration-dependent scattering patterns, a summary of doping experiments using TCNQ, calculated characteristic

ratios, and the assumed energy diagram of thiophene as a function of torsion angle. This material is available free of charge via the Internet at <http://pubs.acs.org>.

AUTHOR INFORMATION

Corresponding Author

*E-mail segalman@berkeley.edu.

Notes

The authors declare no competing financial interest.

ACKNOWLEDGMENTS

Research was supported through the DOE-BES LBL Thermo-electrics Program under Contract DE-AC02-05CH11231. A portion of this research was performed at Oak Ridge National Laboratory's Spallation Neutron Source, sponsored by the U.S. Department of Energy, Office of Basic Energy Sciences. We thank Shrayesh Patel, Adrienne Rosales, Dr. Hannah Murnen, and Prof. Nitash Balsara for helpful discussions.

REFERENCES

- (1) Chow, A. W.; Bitler, S. P.; Penwell, P. E.; Osborne, D. J.; Wolfe, J. F. *Macromolecules* **1989**, *22* (9), 3514–3520.
- (2) Yu, L. P.; Bao, Z. N. *Adv. Mater.* **1994**, *6* (2), 156–159.
- (3) Olsen, B. D.; Segalman, R. A. *Mater. Sci. Eng., R* **2008**, *62* (2), 37–66.
- (4) Hu, D. H.; Yu, J.; Wong, K.; Bagchi, B.; Rossky, P. J.; Barbara, P. F. *Nature* **2000**, *405* (6790), 1030–1033.
- (5) Snyder, C. R.; Henry, J. S.; DeLongchamp, D. M. *Macromolecules* **2011**, *44* (18), 7088–7091.
- (6) Hartmann, L.; Tremel, K.; Uttiya, S.; Crossland, E.; Ludwigs, S.; Kayunkid, N.; Vergnat, C.; Brinkmann, M. *Adv. Funct. Mater.* **2011**, *21* (21), 4047–4057.
- (7) Gettinger, C. L.; Heeger, A. J.; Drake, J. M.; Pine, D. J. *J. Chem. Phys.* **1994**, *101* (2), 1673–1678.
- (8) Gettinger, C. L.; Heeger, A. J.; Drake, J. M.; Pine, D. J. *Mol. Cryst. Liq. Cryst. Sci. Technol., Sect. A* **1994**, *256*, 507–512.
- (9) Adachi, T.; Brazard, J.; Chokshi, P.; Bolinger, J. C.; Ganesan, V.; Barbara, P. F. *J. Phys. Chem. C* **2010**, *114* (48), 20896–20902.
- (10) Hu, D. H.; Yu, J.; Padmanaban, G.; Ramakrishnan, S.; Barbara, P. F. *Nano Lett.* **2002**, *2* (10), 1121–1124.
- (11) Fytas, G.; Nothofer, H. G.; Scherf, U.; Vlassopoulos, D.; Meier, G. *Macromolecules* **2002**, *35* (2), 481–488.
- (12) Meier, H.; Stalmach, U.; Kolshorn, H. *Acta Polym.* **1997**, *48* (9), 379–384.
- (13) Soggi, E. P.; Farmer, B. L.; Adams, W. W. *J. Polym. Sci., Part B: Polym. Phys.* **1993**, *31* (13), 1975–1982.
- (14) Petekidis, G.; Vlassopoulos, D.; Galda, P.; Rehahn, M.; Ballauff, M. *Macromolecules* **1996**, *29* (27), 8948–8953.
- (15) Lu, Y. J.; Weers, B.; Stellwagen, N. C. *Biopolymers* **2001**, *61* (4), 261–275.
- (16) Salaneck, W. R.; Ingnas, O.; Nilsson, J. O.; Osterholm, J. E.; Themans, B.; Bredas, J. L. *Synth. Met.* **1989**, *28* (1–2), C451–C460.
- (17) Aime, J. P.; Bargain, F.; Schott, M.; Eckhardt, H.; Elsenbaumer, R. L.; Miller, G. G.; McDonnell, M. E.; Zero, K. *Synth. Met.* **1989**, *28* (1–2), C407–C417.
- (18) Aime, J. P.; Bargain, F.; Schott, M.; Eckhardt, H.; Miller, G. G.; Elsenbaumer, R. L. *Phys. Rev. Lett.* **1989**, *62* (1), 55–58.
- (19) Anthony, J. E.; Heeney, M.; Ong, B. S. *MRS Bull.* **2008**, *33* (7), 698–705.
- (20) Roncali, J. *Chem. Rev.* **1992**, *92* (4), 711–738.
- (21) Yamamoto, T.; Komarudin, D.; Arai, M.; Lee, B. L.; Suganuma, H.; Asakawa, N.; Inoue, Y.; Kubota, K.; Sasaki, S.; Fukuda, T.; Matsuda, H. *J. Am. Chem. Soc.* **1998**, *120* (9), 2047–2058.
- (22) Adachi, T.; Brazard, J.; Ono, R. J.; Hanson, B.; Traub, M. C.; Wu, Z. Q.; Li, Z. C.; Bolinger, J. C.; Ganesan, V.; Bielawski, C. W.; Bout, D. A. V.; Barbara, P. F. *J. Phys. Chem. Lett.* **2011**, *2* (12), 1400–1404.
- (23) He, Z. R.; Yang, X. Z.; Zhao, D. L. *Macromol. Theory Simul.* **1995**, *4* (2), 277–288.
- (24) Patel, S. N.; Javier, A. E.; Stone, G. M.; Mullin, S. A.; Balsara, N. P. *ACS Nano* **2012**, *6* (2), 1589–1600.
- (25) Vaia, R. A.; Krishnamoorti, R.; Benner, C.; Trimer, M. *J. Polym. Sci., Part B: Polym. Phys.* **1998**, *36* (13), 2449–2459.
- (26) Loewe, R. S.; Ewbank, P. C.; Liu, J. S.; Zhai, L.; McCullough, R. D. *Macromolecules* **2001**, *34* (13), 4324–4333.
- (27) Loewe, R. S.; Khersonsky, S. M.; McCullough, R. D. *Adv. Mater.* **1999**, *11* (3), 250.
- (28) Niemi, V. M.; Knuuttila, P.; Osterholm, J. E.; Korvola, J. *Polymer* **1992**, *33* (7), 1559–1562.
- (29) Kasparkova, V.; Ommundsen, E. *Polymer* **1993**, *34* (8), 1765–1767.
- (30) Zhao, J. K.; Gao, C. Y.; Liu, D. J. *Appl. Crystallogr.* **2010**, *43*, 1068–1077.
- (31) Wignall, G. D.; Bates, F. S. *J. Appl. Crystallogr.* **1987**, *20*, 28–40.
- (32) Debye, P. *J. Phys. Colloid Chem.* **1947**, *51* (1), 18–32.
- (33) Kotlarchyk, M.; Chen, S. H. *J. Chem. Phys.* **1983**, *79* (5), 2461–2469.
- (34) Visser, S. A.; Pruckmayr, G.; Cooper, S. L. *Macromolecules* **1991**, *24* (25), 6769–6775.
- (35) Sharp, P.; Bloomfield, V. A. *Biopolymers* **1968**, *6* (8), 1201–1211.
- (36) Tashiro, K.; Ono, K.; Minagawa, Y.; Kobayashi, M.; Kawai, T.; Yoshino, K. *J. Polym. Sci., Part B: Polym. Phys.* **1991**, *29* (10), 1223–1233.
- (37) Benoit, H.; Doty, P. *J. Phys. Chem.* **1954**, *57* (9), 958–963.
- (38) Mark, J. E. *Physical Properties of Polymer Handbook*, 2nd ed.; Springer: New York, 2006; p xix.
- (39) Brulet, A.; Boue, F.; Cotton, J. P. *J. Phys. II* **1996**, *6* (6), 885–891.
- (40) Dai, L. M. *Eur. Polym. J.* **1993**, *29* (5), 645–651.
- (41) Young, R. J.; Lovell, P. A. *Introduction to Polymers*, 2nd ed.; Chapman & Hall: London, 1991; p x.
- (42) Themans, B.; Salaneck, W. R.; Bredas, J. L. *Synth. Met.* **1989**, *28* (1–2), C359–C364.
- (43) Darling, S. B.; Sternberg, M. *J. Phys. Chem. B* **2009**, *113* (18), 6215–6218.
- (44) Westenhoff, S.; Beenken, W. J. D.; Yartsev, A.; Greenham, N. C. *J. Chem. Phys.* **2006**, *125*, 15.
- (45) Flory, P. J. *J. Chem. Phys.* **1949**, *17* (3), 303–310.
- (46) Bucci, P.; Longeri, M.; Veracini, C. A.; Lunazzi, L. *J. Am. Chem. Soc.* **1974**, *96* (5), 1305–1309.
- (47) Salaneck, W. R.; Ingnas, O.; Themans, B.; Nilsson, J. O.; Sjogren, B.; Osterholm, J. E.; Bredas, J. L.; Svensson, S. *J. Chem. Phys.* **1988**, *89* (8), 4613–4619.
- (48) Wignall, G. D.; Ballard, D. G. H.; Schelten, J. *Eur. Polym. J.* **1974**, *10* (9), 861–865.
- (49) Tenhoeve, W.; Wynberg, H.; Havinga, E. E.; Meijer, E. W. *J. Am. Chem. Soc.* **1991**, *113* (15), 5887–5889.
- (50) Thienpont, H.; Rikken, G. L. J. A.; Meijer, E. W.; Tenhoeve, W.; Wynberg, H. *Phys. Rev. Lett.* **1990**, *65* (17), 2141–2144.
- (51) Klaerner, G.; Miller, R. D. *Macromolecules* **1998**, *31* (6), 2007–2009.